Optical power-driven electron spin relaxation regime crossover in Mn-doped bulk GaAs

F. Münzhuber, T. Kiessling,* W. Ossau, and L. W. Molenkamp
Physikalisches Institut Universität Würzburg, Lehrstuhl für Experimentelle Physik III, Am Hubland, 97074 Würzburg

G. V. Astakhov
Physikalisches Institut Universität Würzburg, Lehrstuhl für Experimentelle Physik VI, Am Hubland, 97074 Würzburg
and A.F. Ioffe Physical-Technical Institute, Russian Academy of Sciences, 194021 St. Petersburg, Russia
(Received 19 May 2015; published 24 September 2015)

We demonstrate tunability of the electron spin lifetime in Mn-doped GaAs by purely optical means. The observed behavior stems from a crossover of the electron spin relaxation rate with increasing excitation density, first decreasing due to the exchange interaction of Mn bound holes with Mn ions, and then increasing again as the valence band is populated and Bir-Aranov-Pikus relaxation sets in. On this account, we explain the complex spatial spin polarization profiles emerging from inhomogeneous optical excitation, which are the result of the combined action of this nonmonotonic spin relaxation characteristics and the intricate photocarrier decay dynamics.

DOI: 10.1103/PhysRevB.92.115208 PACS number(s): 71.55.Eq, 72.20.Jv, 85.75.−d

I. INTRODUCTION

The observation of spin relaxation times in excess of 100 ns of minority electrons in p-type GaAs:Mn has recently renewed the interest in this material system [1–4]. Nonmagnetic p-type GaAs exhibits rapid electron spin relaxation by the Bir-Aranov-Pikus mechanism [5], and because of this p-type, GaAs is generally not considered very attractive for possible spin-based application schemes [6]. The massive enhancement of the electron spin lifetime by p doping with magnetic impurities thus opens a new perspective for p-type systems [1].

The relaxation time prolongation arises from very rapid hole trapping by ionized acceptor states [7] and the antiferromagnetic exchange interaction between Mn ions and Mn-bound holes. In this situation, the spin orientation of the hole spin is locked and the photoexcited electrons cannot relax their spin via scattering with free or bound holes. For sufficiently high excitation densities, the fluctuating fields of ionized magnetic impurities are further compensated and electron spin relaxation is drastically slowed down ($\tau_S > 150$ ns).

The overall electron spin dynamics in such a system is quite complex, mainly because of the minority nature of the electrons. Due to the complete absence of electrons in equilibrium, the decay dynamics of the electrons (rather than the spin relaxation itself) may be limiting the observable spin lifetimes. As the electron lifetime also crucially depends on the exact details of sample composition and excitation conditions [7], necessary to generate an electron population to begin with, an intricate dependence arises between the population of electronic reservoirs and the resultant spin decay mechanisms. This in return provides an additional degree of freedom to drive the spin dynamics.

In this paper, we show how spin relaxation can be tuned from fast to slow and back to fast in GaAs:Mn purely by standard optical means. In a sample, which at low excitation density shows the spin lifetime enhancement discussed above, we demonstrate that strong photo excitation can saturate the Mn acceptors, leading to a sizable population of free and exciton bound holes. In this regime, the average electron lifetime is radically decreased and efficient spin relaxation sets in again by the Bir-Aronov-Pikus mechanism (BAP), both of which result in a very rapid drop of the spin lifetime. We show that an appropriate choice of the intensity profile of the optical excitation enables optical writing of a spin ring structure.

II. MINORITY CARRIER SPIN LIFETIME REGIMES

For the purposes of this report we restrict our measurements to the same sample that was extensively studied in previous work [1]. The main findings have been reproduced for a range of samples of the same material class. The sample was grown by metal organic vapor phase epitaxy (MOVPE) on a (001) oriented GaAs substrate. The GaAs:Mn layer has a thickness of 36 μm and a concentration of Mn acceptors of $N_{\mathrm{Mn}} = 8 \times 10^{17}$ cm^{-3}. The sample is partially compensated, mostly due to unintentional carbon co-doping and Mn interstitials [8].

We start out by identifying the relevant electronic reservoirs by means of standard continuous wave (cw) photoluminescence (PL) spectroscopy. All experiments have been performed in a confocal PL geometry using a He bath cryostat, which is placed between a pair of Helmholtz coils that provides magnetic fields up to 200 mT. A diode laser at $\lambda = 785$ nm (1.58 eV) is used as a source and high excitation intensities are achieved by focusing the laser spot to 18 μm ($\frac{1}{e}$) by an infinity corrected microscope objective (NA = 0.14, $f = 40$ mm), which results in power densities up to 2.5 W cm^{-2}. This is about two orders of magnitude higher than the excitation power density in previous studies [1,3]. Intensities are tuned by neutral density filters to maintain clean beam properties. Spectral resolution is obtained by a standard 1000 mm focal length Czerny-Turner-monochromator equipped with a 1200 mm^{-1} grating and a gateable avalanche photo diode. All data shown in this work have been taken at 8 K in He exchange gas.

The results of the PL experiments are summarized in Fig. 1. In the vicinity of 1.51 eV, we observe donor and acceptor bound excitonic transitions that have merged into a single asymmetric band, as is typical for a material of this doping

*tobias.kiessling@physik.uni-wuerzburg.de

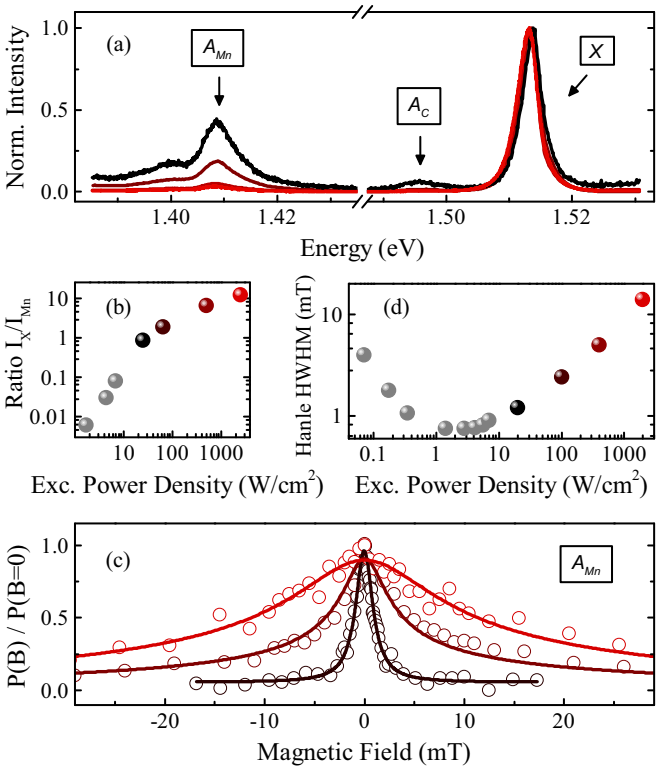

FIG. 1. (Color online) (a) PL spectra evolution as function of excitation power densities (from 20 (black) to 2500 W cm^{-2} (red). The luminescence is increasingly dominated by the excitons. (b) Ratio of the integrated intensities of the excitonic transitions to Mn-impurity related transitions as a function of excitation power. Grey shaded data points are adapted from Ref. [1], other colors correspond to (a). (c) Representative Hanle data recorded at 1.41 eV for excitation intensities of 20 (black), 400 (brown), and 2000 (red) W cm^{-2}. (d) Evolution of the Hanle half-width as a function of excitation density.

density [9]. At about 1.49 eV, we observe a weak band, which is indicative of co-doping by carbon acceptors [10]. Centering around 1.41 eV, we identify the Mn-characteristic luminescence band that consists of (e, A^0_{Mn}) and (D^0, A^0_{Mn}) transitions, which are not resolvable individually [11]. In accordance with our previous work [1], the measurements confirm the trend of increasing spectral weight of the excitonic luminescence with increasing excitation power [see Fig. 1(b)].

We now turn to an investigation of the spin dynamics, employing the Hanle effect in Voigt geometry [12]. We use standard optical orientation to generate a nonequilibrium spin density. Earlier experiments have shown that the polarization signal of the A^0_{Mn} line in a transverse magnetic field can be unambiguously attributed to the electron spin in a bulk material as ours [3]. To avoid optical orientation by the nuclei and to suppress Overhauser fields, we use a photoelastic modulator to change the sign of the excitation from σ^+ to σ^- helicity with a frequency of 50 kHz. Using a quarter-wave plate/Glan-Thomson-prism assembly in the detection path, we measure the intensity I^+_+ (I^+_-) of the σ^+ PL after the σ^+ (σ^-) excitation with a gateable photon counter. The spin polarization S_z is proportional to the polarization P of the luminescence, which can be calculated according to $P = (I^+_+ - I^+_-)/(I^+_+ + I^+_-)$. In this configuration, the response of the photoinitialized spin polarization $S_Z(0)$ to an applied transversal magnetic field in the absence of diffusion follows the relation [12]

$$S_Z(B) = \frac{S_Z(0)}{1 + (\omega_L T_S)^2} \; (\propto P(B)) \tag{1}$$

with ω_L the Larmor frequency. The width of the Lorentz shaped Hanle curve is therefore reciprocal to the spin lifetime T_S, which itself is given by

$$T_S^{-1} = \tau_S^{-1} + \tau_L^{-1}, \tag{2}$$

in which τ_s is the electron spin relaxation time and τ_L is the electron lifetime. We will show later that the spatial intensity profile of the PL proves lateral diffusion to be negligible, which is a consequence of the small low-temperature electron mobility in highly doped bulk GaAs. Vertical diffusion inside the sample may occur, but probing at the energy of the deep Mn acceptor allows us to use the Hanle width as a tool for determining the electron spin lifetime even in this case [13]. Further, fast exchange scattering between electrons of all involved electronic reservoirs ensures that the level of spin polarization is kept equivalent for exciton bound electrons and band electrons [14,15].

Representative Hanle curves are given in Fig. 1(c). For an excitation power density around 10 W cm^{-2}, we reproduce the previous result of a remarkably long spin relaxation time τ_S [1], which is caused by the hole spin locking to the spin of the Mn acceptor and the concomitant suppression of the fluctuations of the localized magnetic moments. As the power density is increased, we observe a strong broadening of the Hanle curves, corresponding to a drastic decrease of the electron spin lifetime. The overall evolution of the latter is summarized in Fig. 1(d).

We attribute the drastic increase in the HWHM of the curves to two accompanying processes, each of which is responsible for the shortening of one contribution to T_S. To quantify our interpretation, we employ in the following a recently published model of the recombination dynamics in a sample such as ours [7]. Without going into the details (for which the reader is referred to the original work), we briefly summarize the fundamental ideas.

It is well understood from time-resolved PL studies that there is a pronounced dependence of the reservoir populations and their decay dynamics on the excitation conditions. This is due to the two competing recombination channels for photoexcited electron-hole pairs.

First, charge carriers can recombine directly through excitonic transitions, which happen on the time scale of the radiative exciton lifetime τ_X. Second, holes can be captured by charged acceptors and the remaining electrons subsequently recombine with the neutralized impurities.

For a quantitative description of the latter we use a model based on Shockley-Read-Hall recombination [16,17], in which the capture time $\tau_{\mathrm{cap},i,J}$ of a charge carrier i by an impurity J is given by the thermal velocity $v_{\mathrm{th},i}$, the number of available trapping centers N_J, and the cross section of the trapping center $\sigma_{i,J}$:

$$\frac{1}{\tau_{\mathrm{cap},i,J}} = \sigma_{i,J} v_{\mathrm{th},i} N_J. \tag{3}$$

While this expression is rather simple, the solution for the capture time τ_{cap} of a single charge carrier is fairly complex due to the large number of different recombination centers in the sample that have to be considered for realistic modeling.

The decay of the exciton population dn_X/dt directly couples the excitonic recombination dynamics to the occupation of the available electron reservoirs by

$$\frac{dn_X(t)}{dt} = G_X(t) - \frac{n_X(t)}{\tau_X} - \sum_{i,J} \frac{n_X(t)}{\tau_{\text{cap},i,J}(t)} \tag{4}$$

with G_X being a generation term.

Quantitative modeling of the exciton decay time thus requires solving the full set of coupled rate equations in order to obtain its temporal evolution and its excitation power dependence, which includes excitons, free band electrons and holes, shallow donors, carbon, and manganese acceptors.

For the cw situation of this work, G is obviously proportional to the excitation power density and temporally constant. We then obtain the photoexcited electron density n_e by adding up the populations of all possible reservoirs in which electrons may reside before recombination, i.e., band states, excitons, and donor bound electrons. In Fig. 2(a), we show the resulting nonlinear increase in n_e with increasing excitation power.

Using the continuity equation for carrier concentrations in excited semiconductors, we can finally obtain the averaged electron lifetime τ_L from n_e by [18]

$$\tau_L = \frac{n_e}{G}. \tag{5}$$

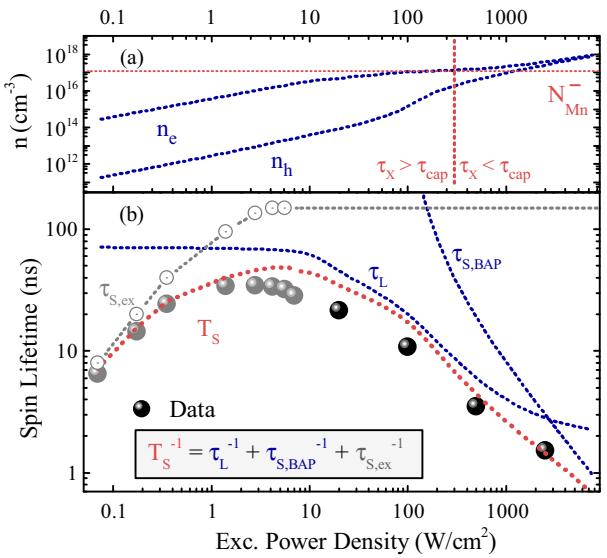

FIG. 2. (Color online) (a) Population densities of electronic reservoirs as a function of the excitation density modeled from PL. Indicated are the overall electron density n_e, the added density of free and exciton-bound holes n_h (as only these contribute to BAP relaxation), and the density of available ionized Mn acceptor states. The vertical line marks the transition from dominating hole capture by acceptor states to dominating hole decay by excitons, assigning the onset of a sizable hole population capable of BAP scattering. (b) Evolution of the electron spin lifetime T_S with excitation density. Grey dots mark previously published data points [1]. For details of modeling see text.

Taking everything together and comparing the evolution of the spin lifetime T_S with the charge carrier populations in Fig. 2, we directly see that the onset of the decrease of T_S is determined by the decrease in τ_L. Moreover, this happens right in the regime in which we identify a distinct kink in the evolution of n_e.

Both observations are straightforward to understand. In the low excitation limit, photoholes are rapidly captured onto empty acceptor states that are available due to the partial compensation of the sample. As such, long-lived Mn-impurity related transitions [(e, A^0_{Mn}) or (D^0, A^0_{Mn})] are prevalent and only a negligible number of exciton transitions occur, so the electron lifetime in this regime is long.

As the excitation density is increased, the acceptor states are gradually driven towards saturation. The residual holes then start recombining as excitons which accordingly gain sizable spectral weight, as can be seen in Fig. 1(b). Since the excitonic lifetime τ_X is short compared to Mn-impurity related decay times, the *average* electron lifetime decreases.

Our model further yields the density of free and exciton-bound holes, the sum of which is also shown in Fig. 2(a). [19] As a sizable population of nonlocalized holes becomes available, BAP relaxation starts setting in, which further accelerates the spin decay. The relaxation rate by the BAP mechanism can be approximated by

$$\frac{1}{\tau_{S,\text{BAP}}} = v_{\text{th},e}\sigma_{eh}n_h \tag{6}$$

with σ_{eh} the scattering cross section of electrons with holes [6], and n_h the combined density of free and exciton bound holes. By extracting the number of holes in these two reservoirs from the experimentally calibrated rate equations (see above), we are finally in a position to quantitatively model the overall evolution of the electron spin lifetime T_S. The thermal velocity of the electrons $v_{\text{th},e}$ is taken to be a constant at 25 K. Previous studies demonstrated that even for the strong pumping conditions used in this work, the electron temperature will not increase much further as the emission of optical phonons at electron temperatures above this value is enhanced and provides a very effective cooling channel [20].

Taking the values for the spin lifetime T_S resulting from the modeled τ_L and $\tau_{S,\text{BAP}}$ as well as the values for $\tau_{S,\text{ex}}$ and comparing them to our experimental data, we find excellent agreement as is shown in Fig. 2(b). [21]

III. SPATIAL SPIN POLARIZATION PROFILES

The nonmonotonic dependence of the spin lifetime on optical intensity has strong implications on the spatial pattern of the spin profile upon local excitation. The nonhomogenous excitation power profile of a tightly focused laser beam directly translates into a spatially dependent spin polarization profile. We demonstrate by means of spatially resolved PL that the resulting spin pattern is well described by our above model, corroborating the validity of our analysis.

The Gaussian intensity profile of the laser beam results in a power density at the center of excitation which is several orders of magnitude stronger than in regions some 10 μm away from the center. Following the trend shown in Fig. 2(b), we expect very different spin lifetimes in these regions.

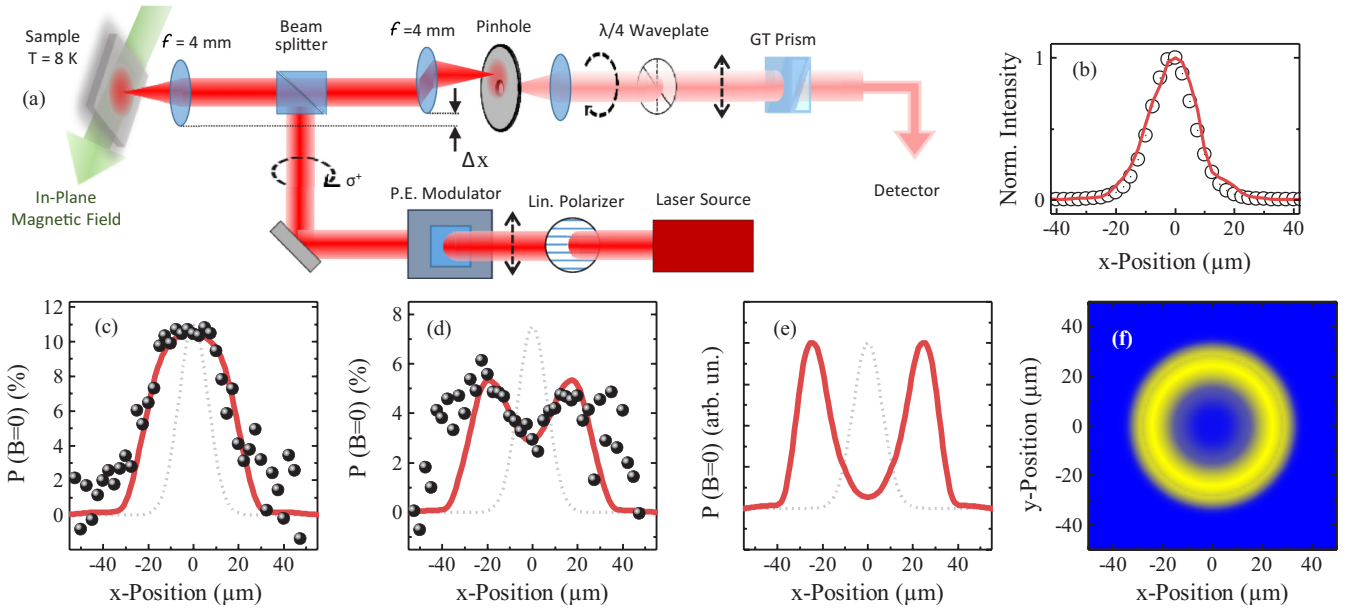

FIG. 3. (Color online) (a) Detection scheme to measure spatially and polarization-resolved PL. (b) Spectrally integrated lateral PL intensity profile (black) compared to laser excitation profile (red). (c) Measured local PL polarization at 1.41 eV (black dots, $P_{\mathrm{exc,Max}} = 200\,\mathrm{W\,cm^{-2}}$) and modeled polarization profile in red line in case of medium excitation power. The excitation intensity profile is indicated in grey dotted line. (d) Same as in (c) but with a peak power density of 5000 $\mathrm{W\,cm^{-2}}$. (e) Modeled polarization profile with peak excitation power density $P_{\mathrm{exc}} = 100\,\mathrm{W\,cm^{-2}}$, which means a thirteen fold increase compared to (d). (f) Two-dimensional lateral polarization profile according to the model used in (e). Color encoding links yellow to high and blue to low values for polarization.

In order to measure the local spin polarization, we insert a pair of confocal lenses in the detection path with a fixed pinhole ($d = 10\ \mu$m) placed in their common focal plane [see Fig. 3(a)]. Lateral scanning of the lens in front of the pinhole displaces the image of the sample surface in the common focal plane. We can hence control the area of the sample surface of which luminescence is transmitted through the pinhole and finally detected, which enables us to map the polarization profile.

We do not observe spatial photocarrier diffusion in the studied excitation power regime, as is evidenced by the spatial overlap of the integrated PL profile with the profile of the excitation laser [Fig. 3(b)]. We can thus validate the premise of omitting diffusion in the spin decay modeling.

The resultant local PL polarization profile of the focused excitation beam is shown in Fig. 3(c). The intensity is chosen to maximize the polarization at the center of excitation.

We can model the observed spatial pattern by translating the local excitation power density into a local spin lifetime $T_S(x)$ and charge carrier lifetime $\tau_L(x)$ according to Fig. 2. The final convolution of the resulting local polarization profile [12]

$$P(x) \propto \frac{T_S(x)}{\tau_L(x)} \tag{7}$$

with the apparatus function of the pinhole reproduces the measured profile well and is also shown in Fig. 3(c). It is worth noting that the actual spin polarization is twice as large as the optical polarization due to optical selection rules [12].

The model correctly predicts the spatial evolution of the spin profile with increasing excitation density as is shown in Fig. 3(d). The stronger excitation translates into a further reduced spin lifetime at the center of excitation that is framed by a symmetric region of long spin lifetimes, which then again decreases for larger distances. This is in clear contrast to Fig. 3(c), in which the low excitation intensity only yields a plateau of high polarization.

While we cannot experimentally access higher excitation densities, our model predicts a great deal of tunability of the achievable spin pattern, as is shown in Figs. 3(e) and 3(f). Upon very hard pumping, it is possible to shift the region of high polarization away from the center of excitation and increase the contrast between the center of the ring and the region of high spin polarization. Further, in this regime, one can completely remove the spin information locally by purely optical means.

IV. CONCLUSION

We demonstrate that photopumping of partially compensated Mn-doped p-type GaAs enables a regime crossover in the minority electron spin lifetime. Extending the previously observed rise in τ_S for low excitation density to the high-density regime, we observe the onset of very fast electron spin relaxation, the position of which is determined by the degree of compensation. The decrease in T_S arises from the complete neutralization of the Mn acceptor reservoir, which results in a reduction of minority electron lifetime by then predominant excitonic recombination and concomitant BAP relaxation.

The plateau of the long electron spin lifetime can be translated into a spatially varying spin polarization degree for strongly focused optical excitation, as evidenced by the

comparison of spatially resolved experiments and our model calculations. This allows for pure optical modulation of spatially nonmonotonic spin polarization profiles within the material.

ACKNOWLEDGMENTS

The authors thank V. L. Korenev for very fruitful discussions and gratefully acknowledge financial support from the DFG (OS 98/9-3, SPP1285), the EU ERC-AG (Project 3-TOP), and the RSF (Grant No. 14-42-00015).

[1] G. V. Astakhov, R. I. Dzhioev, K. V. Kavokin, V. L. Korenev, M. V. Lazarev, M. N. Tkachuk, Yu. G. Kusrayev, T. Kiessling, W. Ossau, and L. W. Molenkamp, Suppression of Electron Spin Relaxation in Mn-Doped GaAs, Phys. Rev. Lett. **101**, 076602 (2008).

[2] I. A. Akimov, R. I. Dzhioev, V. L. Korenev, Yu. G. Kusrayev, V. F. Sapega, D. R. Yakovlev, and M. Bayer, Electron spin dynamics and optical orientation of Mn ions in GaAs, J. Appl. Phys. **113**, 136501 (2013).

[3] I. A. Akimov, R. I. Dzhioev, V. L. Korenev, Yu. G. Kusrayev, E. A. Zhukov, D. R. Yakovlev, and M. Bayer, Electron-spin dynamics in Mn-doped GaAs using time-resolved magneto-optical techniques, Phys. Rev. B **80**, 081203 (2009).

[4] R. C. Myers, M. H. Mikkelsen, J.-M. Tang, A. C. Gossard, M. E. Flatte, and D. D. Awschalom, Zero-field optical manipulation of magnetic ions in semiconductors, Nat. Mater. **7**, 203 (2008).

[5] G. L. Bir, A. G. Aronov, and G. E. Pikus, Zh. Eksp. Teor. Fiz. **69**, 1382 (1975) [Sov. Phys. JETP **42**, 705 (1976)].

[6] Guy Fishman and Georges Lampel, Spin relaxation of photo-electrons in p-type gallium arsenide, Phys. Rev. B **16**, 820 (1977).

[7] F. Münzhuber, T. Henn, T. Kiessling, W. Ossau, L. W. Molenkamp, B. Gieseking, G. V. Astakhov, and V. Dyakonov, Exciton decay dynamics controlled by impurity occupation in strongly Mn-doped and partially compensated bulk GaAs, Phys. Rev. B **90**, 125203 (2014).

[8] Steven C. Erwin and A. G. Petukhov, Self-Compensation in Manganese-Doped Ferromagnetic Semiconductors, Phys. Rev. Lett. **89**, 227201 (2002).

[9] W. Schairer and M. Schmidt, Strongly quenched deformation potentials of the Mn acceptor in GaAs, Phys. Rev. B **10**, 2501 (1974).

[10] D. J. Ashen, P. J. Dean, D. T. J. Hurle, J. B. Mullin, A. M. White, and P. D. Greene, The incorporation and characterisation of acceptors in epitaxial GaAs, J. Phys. Chem. Solids **36**, 1041 (1975).

[11] T. C. Lee and W. W. Anderson, Edge Emission involving Manganese Impurities in GaAs at 4.2 K, Solid State Commun. **2**, 265 (1964).

[12] *Optical Orientation*, edited by F. Meyer and B. P. Zakharchenya (North-Holland, Amsterdam, 1984).

[13] R. I. Dzhioev, B. P. Zakharchenya, R. R. Ichkitidze, K. V. Kavokin, and P. E. Pak, Spectral dependence of the hanle effect due to diffusion of optically oriented electrons in p-type semiconductors, Phys. Solid State **35**, 1396 (1993).

[14] Daniel Paget, Optical detection of nmr in high-purity gaas under optical pumping: Efficient spin-exchange averaging between electronic states, Phys. Rev. B **24**, 3776 (1981).

[15] K. V. Kavokin, Spin relaxation of localized electrons in n-type semiconductors, Semiconductor Sci. Technol. **23**, 114009 (2008).

[16] W. Shockley and W. T. Read, Statistics of the recombinations of holes and electrons, Phys. Rev. **87**, 835 (1952).

[17] J. S. Blackmore, *Semiconductor Statistics*, Vol. 3 (Pergamon Press, Oxford, 1962).

[18] S. M. Sze and K. K. Ng, *Physics of Semiconductor Devices*, 3rd ed. (Wiley, New York, 2007).

[19] Including acceptor bound photoholes the number of total electrons and holes is of course equal for all excitation conditions, but it will become clear in following why those are excluded for the identification of the dominant spin decay mechanisms.

[20] T. Kiessling, J.-H. Quast, A. Kreisel, T. Henn, W. Ossau, and L. W. Molenkamp, Spatially resolved photocarrier energy relaxation in low-doped bulk GaAs, Phys. Rev. B **86**, 161201 (2012).

[21] Deviations at medium excitation power may arise from unaccounted spin relaxation contributions of holes bound to non magnetic impurities or Dyakonov-Perel mechanism.